11th International Conference on Fracture Mechanics of Concrete and Concrete Structures
FraMCoS-11
J. M. Chandra Kishen, A. Ramaswamy, S. Ray and R. Vidyasagar (Eds)
https://doi.org/10.21012/FC11.092356

A NEW PERSPECTIVE ON CRACK INSTABILITY OF SPALLING CONCRETE IN FIRE

Ramin Yarmohammadian*[1] **Roberto Felicetti**[1] **and Patrick Bamonte**[1]

* Politecnico di Milano (POLIMI)
Piazza Leonardo da Vinci, 32, Milano, Italy , CAP:20133
e-mail: ramin.yarmohammadian@polimi.it

Key words: Fire-induced spalling, High temperature, Pore pressure

Abstract: Explosive spalling keeps being one of the main open issues concerning the fire safety of concrete structures. Though it is recognized that cracks in the exposed cover can be triggered by the combined effect of thermal stress and pore pressure, the energy source and the mechanism behind the violent projection of fragments are not yet fully understood. Nonetheless, the huge thermal energy accumulated in the hot cover (in the order of 500kJ/m^2 in a 1mm thick layer) has a high potential to drive dynamic fracturing, provided that water vaporization could quickly convert it into mechanical work. To make this possible, flash vaporization of a significant amount of water should take place in a sub-millimetre layer facing the opening crack (since vapour diffusion time goes with the path length squared).

To validate this new perspective, a special setup was developed where concrete disks (D=100mm, thickness=60mm) were heated on the two opposite faces, so to instate a thermo-hygral transient similar to the concrete cover exposed to fire, while keeping negligible the contribution of thermal stress. A crack is triggered in the sample mid-plane by the high thermal dilation of a polymeric insert (a PTFE ring) embedded in the sample. FEM analyses were performed to optimize the specimen shape and to adjust the insert thickness to control the temperature at which the crack develops a critical opening. Remarkably unstable blasts were observed in high-performance concrete samples, during which the relative acceleration of the two splitting halves was monitored via optical sensors. The results showed that pressure not far from the saturation value quickly develops in the opening crack. Continuous monitoring of the specimen mass also allowed assessing the amount of vaporized water entailed by the process. Tests on pre-dried samples exhibited a milder blast or even a stable propagation of the crack.

In summary, this study is expected to cast new light on the fundamental mechanism behind the explosive spalling phenomenon.

1 INTRODUCTION

There is no doubt that concrete will continue to be utilized as a construction material much into the future as it is now the most often used building material [1]. Thanks to its low conductivity, it is known to exhibit good behaviour in fire. However, the fact that concrete is prone to the spalling phenomenon when exposed to fire poses a significant obstacle to its widespread utilization. Both normal-grade concrete and more recent high-performance and self-compacting concrete may be affected by this issue. Although the latter varieties have better mechanical and durability performance, which allows for more sophisticated designs and a reduction in the structural volume, their susceptibility to spalling is also higher.

In literature, spalling in fire is defined as a violent or non-violent detachment of fragments from the heated concrete surface

[2]. It is a complex phenomenon entailing the thermal, mechanical and hygral material behaviour at high temperatures. The close interconnection of processes dealing with such different branches of applied physics is not yet fully understood and may sometimes lead to contradictory indications [2]. In general, this phenomenon can be explained by the ensuing pore pressure and thermal stress.

From the pore pressure perspective, spalling happens when the effective tensile stress induced by pore pressure is higher than the tensile strength of concrete. This mechanism is more associated with the thermo-hygral process in heated concrete when the pore pressure exceeds the tensile strength of concrete [3–7]. therefore, it has been proved that the pore pressure is ineffective in high-performance concrete, due to the poor interconnection of the pores [8,9]. The thermal stress mechanism claims that thermal gradients and restrained thermal dilation are accounted [8–10], since they may lead to the buckling of the hot skin in the exposed element.

Unfortunately, the discussion on the sensitivity to each distinct influencing parameter does not allow for the formation of a clear picture of the fundamental mechanisms behind this phenomenon, to the point that a quantitative assessment of their role in such unstable concrete fracturing is not yet possible.

A third theory that integrates the aforementioned mechanisms is also present [11–13]. Following this latter line of reasoning, two stages can be recognized in the progress of the phenomenon:

- Incipient crack formation
- unstable crack propagation

In the first stage, high compressive stress parallel to the heated face, fostered by external loads and combined with the orthogonal tension induced by pore pressure[15], can trigger a fracture. Other promoting factors are mesoscale heterogeneity [15], discontinuity caused by rebars and stress unbalance due to the local convex shape (e.g. corners) [16]. Stable cover delamination is frequently observed in post-fire assessment of concrete elements seemingly not affected by spalling [17] which means sometimes the process can be stopped in the first stage. In the case of a highly unstable fracture, searching for the underlying energy source is a crucial step toward understanding the fundamental mechanism and its influencing parameters. Both elastic energy from thermal stress and thermal energy from sensible heat may be present in the hot cover, but most research to date has concentrated on the former. The range of developed kinetic energy (0.5-2.0 kJ/m^2) can be estimated through velocity measurements on spalled splinters of a known thickness [18]. The energy needed to repeatedly fracture the cover should also be added to the balance (0.5 kJ/m^2, based on the typical size of the splinters [19]). However, the total elastic energy stored in a 20 mm layer at 200°C is just about 1 kJ/m^2 [20], whereas the sensible heat accumulated by the same layer is more than 10000 times larger. This is substantiated by the remarkable net thermal flux penetrating the exposed cover (25-50 kW/m^2 in the early stages of fire Figure 1). It is then clear that thermal energy is a prominent candidate to drive the unstable dynamic fracture characterizing explosive spalling, on

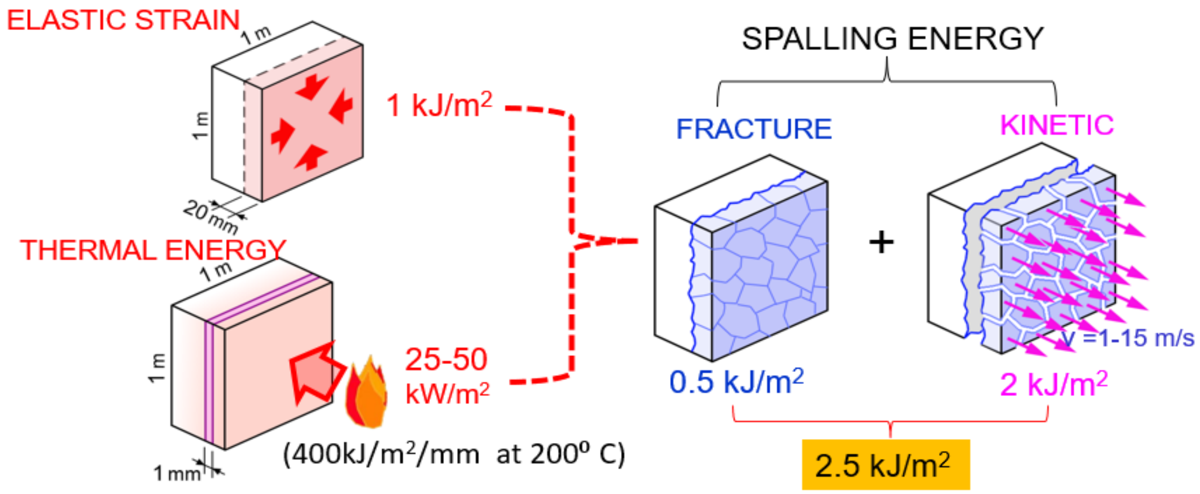

Figure 1: Comparison between stored elastic and thermal energy in heated concrete cover

condition that water vaporization can effectively transform this source into mechanical work. This entails a very fast flow of vapour into the opening crack. Given the low permeability of concrete, a short diffusion path is required (the diffusion time goes with the distance squared). Assuming that 3% by mass of moisture from a 0.1 mm layer on both faces of the fracture (14 g/m^2) is vaporized at 200°C and allowed to expand adiabatically from saturation (1.45 MPa) to ambient pressure, the developed work is 3.5 kJ/m^2, which is consistent with the energy involved in fracture and fragment acceleration.

In the following sections, A novel setup is proposed to analyze how thermal energy and pore saturation contribute to the unstable crack propagation in hot concrete.

2 TEST SETUP

In this new test, a crack is triggered under the minor influence of thermal stress. To accomplish this, a polymeric insert is placed during casting in the midplane of a concrete disk. The high thermal dilatation of polymers and the correct shape and thickness selection for the insert allow the heated samples to be split into two halves. In this paper, PTFE rings of different thicknesses (0.5, 1.0, 1.5, and 2.0mm) were utilized to investigate the effect on the crack onset. The mass loss and the relative acceleration of the two pieces provide indications of the amount of water involved in the process and the effective pressure developed while opening the crack. As it is shown in Figure 2, samples are heated by two opposite radiant heaters fitted with an internal thermocouple for power control.

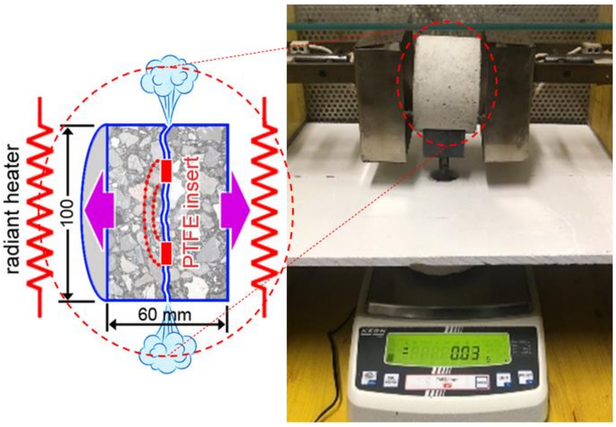

Figure 2: Test setup configuration with the polymer insert within the disk samples

2.1 Mix design

A spalling-sensitive concrete mix was used in the crack instability tests. After casting, all samples were stored in moist conditions and tested after 90 days.

Table 1: Mix proportions

	SP mix
Cement CEM III	400
Filler	280
Sand 0-4 mm	920
Gravel 4-10 mm	630
Effective water	160
w/c	0.4
Max aggregate size	10
Plasticizer (%cement weight)	2.2%
Age at testing [day]	90

Concrete strength class= C80

2.2 Specimen preparation and insert

The polymer ring was positioned in the middle of the disks by casting the samples (D=100mm, h=60mm) in two stages. Sample and ring geometry were optimized based on FEM stress analyses, so to increase the likelihood of generating a planar crack in the midsection, rather than radial cracks or conical punching splinters [21]. As a consequence, the cover of the polymeric insert (30mm) turned out to be thicker than the typical fractured splinters observed in real spalling events (5-20mm, [19]).

Figure 3: Placing the polymer insert (PTFE) during casting and broken half of a tested sample.

2.3 Heating curves

A thicker cover requires longer heating and drying durations because of the time scale dependence on diffusive phenomena. Since a time derivative depends on second spatial derivatives in both the Darcy and Fourier equations, 4 times slower heating should be implemented in a double-thickness layer to instate similar pressure and temperature profiles For this reason, a slowed-down version of the standard fire curve was adopted as a reference to drive the radiant heaters. A heating rate closer to the standard was also implemented to produce more critical conditions in inherently stable situations (like pre-dried samples).

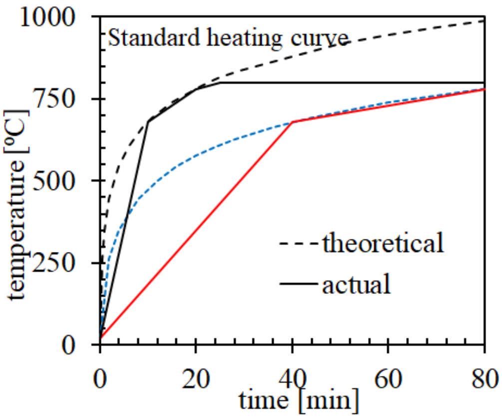

Figure 4: heating curves followed by the two radiant heaters.

3 MEASURING SYSTEMS

3.1 Mass measurements

The exposed samples were supported by an insulating holder placed on a precision balance allowing real-time streaming of mass measurements through a digital port (5 scans/s). The balance is screened from radiation by a gypsum fiberboard and the whole setup is enclosed in a laminar flow box, so to draw any smoke produced by the heated polymeric inserts. The continuous monitoring of the sample mass during the heating process provides two types of results: the global drying experienced by the sample at the time of spalling and throughout the heating test, and the sudden mass loss due to the explosive splitting of the disks.

3.2 Displacement sensing by photosensors

Two reflective photosensors (Vishay CNY70) mounted astride the potential fracture plane were used to monitor the relative displacement between the two separating parts of the breaking disk (Figure 5). The advantage of using this type of sensor are:

- Fast response (cut-off freq. ≈ 20kHz)
- Low cost (≈ 1€)
- Low mass (0.7g)

The current driven by the detector into a resistive load is proportional to the amount of infrared light reflected by a reflective target facing the sensor, which is related to their mutual distance. This relationship is not linear, with the highest sensitivity in the near range (approximately 1V/mm), which aids in monitoring the early stages of crack opening. Very flexible 0.1 mm enamelled copper wires were used for connections to the data logger, with no influence on weight monitoring. Both the sensor and the target were firmly held at some distance from the specimen (70mm) using two stainless steel triangular trusses fixed on two sides of the concrete disks. The central second derivative finite difference method was used to calculate the relative acceleration experienced by the halves of the disk during a spalling event. Under the assumption of splitting into equal masses M/2, the internal force separating the two halves may be calculated using the second Newton's law of motion (separating force = M/2 x relative acceleration/2). Since the tested samples accumulate little elastic energy due to thermal stress, the net separation force is considered to result from the difference between the pressure of vapour filling the crack and the remaining cohesive tensile stress of fracturing concrete. Despite the presence of the ring and the continuously growing cracked region, the nominal cross-section area is used here to convert the total force into the mean stress/pressure.

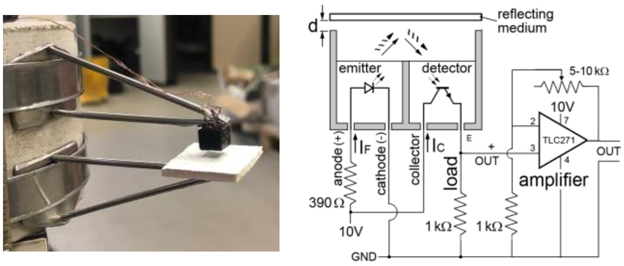

Figure 5: Left: photosensor facing the painted balsa wood target and circuit driving the sensor.

4 RESULTS

In the following, the results regarding different thicknesses of the polymeric ring are presented. Then, the impact on the crack stability of different moisture contents is investigated.

4.1 Effect of insert thickness

These preliminary tests aimed to determine whether the polymer could induce the crack in the same temperature range as the actual phenomenon. Early or delayed crack development would result in an incorrect reproduction of the spalling conditions. Four different thicknesses of the polymeric insert (at least 4 tests for each) have been investigated in the preliminary tests under the four times slowed-down heating curve relative to the standard fire. K-type thermocouples were placed in the midsection of some of the samples to monitor the temperature at which a through crack developed.

The time/ temperature range in which this occurs determines the concurrent saturation and pressure in the pores. Inherent material properties like permeability and fracture brittleness also govern the stability of the process. Among the 4 samples with the thickest polymer insert (2mm), just one exploded with a mild event after about 2300 s heating. At that time, the temperature in the cracking region was just 140-150ºC, entailing a limited amount of thermal energy for driving water vaporization The most realistic temperature range can be obtained with the thinnest PTFE inserts (0.5mm), though at the cost of the increased scatter of results.

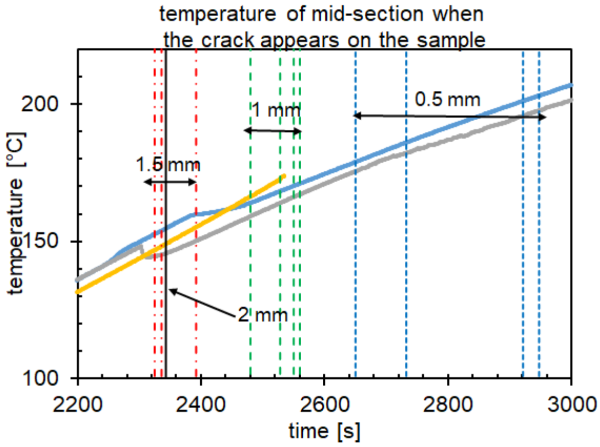

Figure 6: Crack opening time and temperature for different polymer inserts.

In the case of dry concrete, thermal dilation of the polymeric ring allows a stable propagation of a planar crack up to the lateral surface of the concrete disks. On the other hand, the concurrent effect of pore pressure can foster the crack onset and promote the following unstable propagation.

To understand the combined role of the polymer insert and the pore pressure in the initiation of the crack (the first stage of spalling), FEM modelling was performed in ABAQUS software. A soil model is used in order to have the possibility to introduce the effective pore pressure within the samples. Pore pressure was only defined in the vicinity of the crack and in areas that won't be impacted by the drying process in order to create a more realistic model (see Figure 7). The effective pore pressure employed in the model is saturated pore pressure multiplied by Biot's number. This value ranges from 0.25 to 1 depending on the extent of damage and the connectivity of the pore [22]. Using the damage plastic model for the constitutive law of concrete and thermal properties defined in EC2 in the axisymmetric model, the effective pore pressure required for unstable crack propagation is reported as a function of time in Figure 7 for the 0.5mm polymer ring. It is worth noting that higher pore pressure in the model helped the crack to be initiated earlier and pore pressure alone can trigger the crack without any other help. The scattered cracking time in the experiment is seen by removing not realistic pore pressures that are higher than saturated pore pressure in that region.

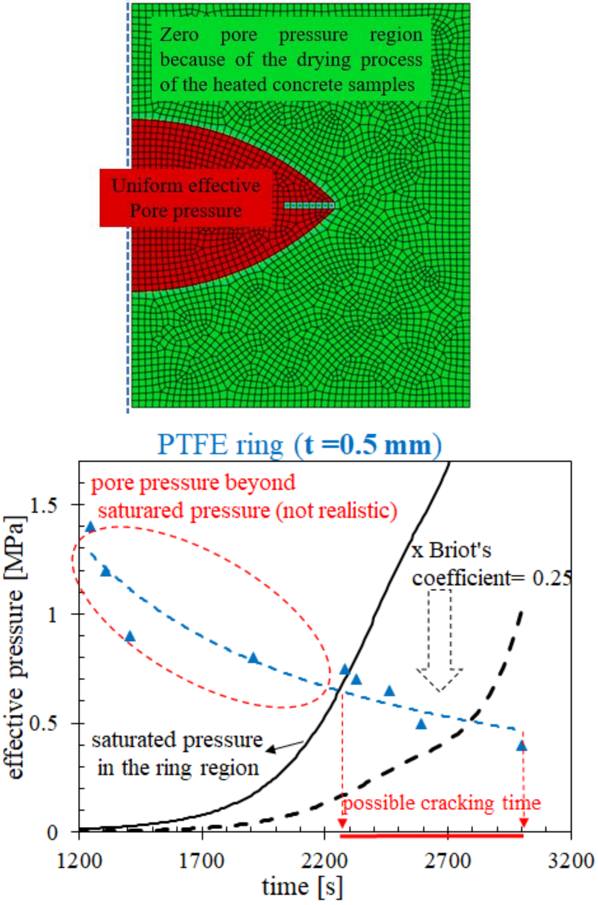

Figure 7: Different effective pressure and the cracking time for 0.5 thickness samples.

Temperature and saturation at the midsection also influence the sudden mass loss observed during spalling. The higher the temperature, the more thermal energy is available to drive vaporization, within the limits allowed by the amount of water in the pores facing the crack. The observed range is 50-200g/m^2, not including some outliers affected by the loss of small concrete fragments.

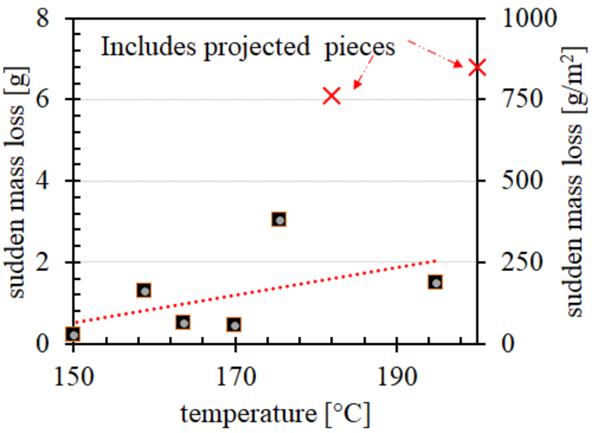

Figure 8: Sudden mass loss versus spalling temperature.

4.2 Effect of initial moisture content

The next step was to batch 6 samples with the selected polymer thickness (0.5mm) and cure them in a 90%RH chamber for 6 months. Three samples were then dried for 45 days at 60°C to minimize the mechanical impacts of concrete shrinkage and insert dilation. The average mass loss was 2.8%, which is about half of the total water released in the tests on moist samples. To create a more severe condition, a heating curve equivalent to the typical fire was implemented through the radiant heaters. All three moist samples spalled, whereas just one of the pre-dried ones did (Figure 9). The lateral face of the non-spalled samples exhibited a visible crack, but the two halves were still linked together. According to the mass loss measurements, these samples were still retaining some water, though not enough to drive a blast. This confirms the importance of pore saturation in concrete spalling.

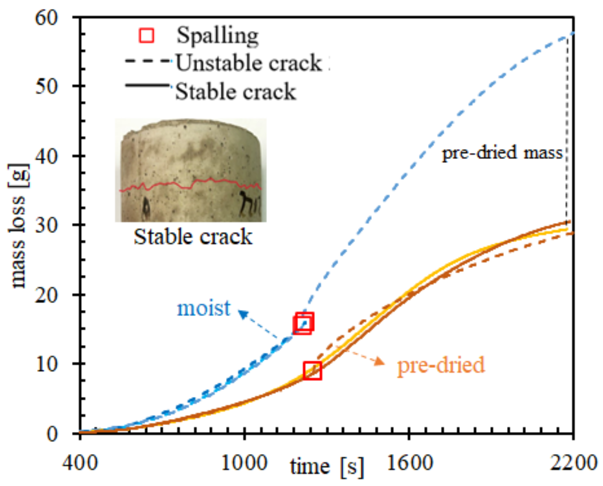

Figure 9: Mass loss of moist and dried samples

In Figure 10, the drying rates observed in the same tests are reported. The sharp increase occurring at the onset of the crack indicates the amount of moisture being released by the freshly exposed material (not including the finite quantity discharged in case of the blast). The common bend observed in both stable and unstable pre-dried samples indicates that comparable pressures, close to the material capacity, should have been produced by the vapour streaming in the incipient cracks.

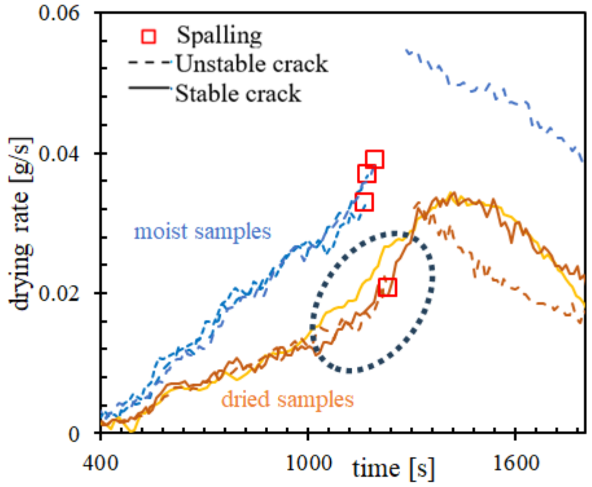

Figure 10: Drying rate of different samples in time.

As discussed, the pressure developed in the blasted samples can be deduced from the relative acceleration between the separating halves of the broken disks (Figure 11). A steep rise is observed up to the critical opening of the crack, beyond which no significant cohesive stress is bridging the fracture. A milder transition is observed in the pre-dried sample. The peak values are in the range of saturated steam pressure at 180-210°C, confirming the pivotal role of pore pressure in crack instability. To be mentioned that the measured peak acceleration is in the order of 10^4m/s^2 and is reached in about 0.1ms, confirming the challenging requirements for the displacement sensors. Pressure then decreases when the flow through the open crack prevails on the vaporization rate at the fractured faces.

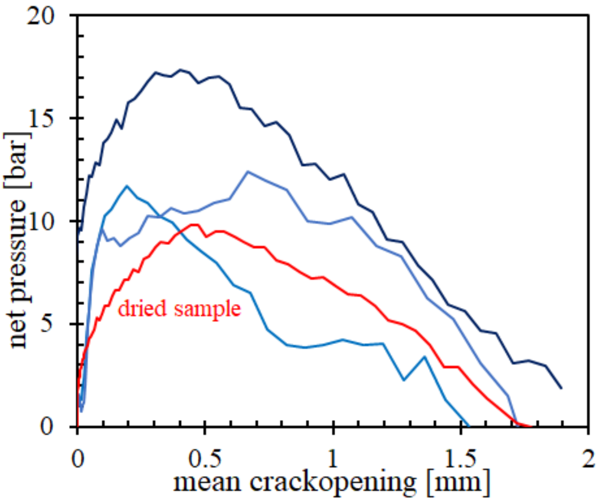

Figure 11: Net pressure versus crack opening in different samples with the same thickness and different moisture content.

6 CONCLUSIONS

The objective of this research is to provide new insight into how thermal energy and rapid water vaporization contribute to the explosive spalling that results from concrete exposure to fire. To achieve this, a novel setup was created in which the thermal expansion of a polymeric insert causes a planar crack to form in a heated concrete disk with little contribution of thermal stress due to temperature gradient. A numerical analysis was conducted to determine the joint effect of the polymer insert and pore pressure buildup in the crack initiation stage. Finally, samples with different initial moisture contents were tested to determine the dual involvement of moisture in both crack initiation and its unstable propagation. A summary of the main conclusions of this study is given in the following:

- Pore pressure can hardly cause the crack to form alone. However, if a crack is triggered by a stable mechanism (thermal expansion), the effect of pressure is to make the fracture considerably unstable.
- The time at which a crack is triggered is critical. Due to insufficient thermal energy or pore saturation, early and late cracks are more stable. The most severe spalling occurs when hot concrete retains sufficient moisture in the pores.
- Lower spalling risk is observed in dried samples when the pores facing an incipient crack are not able to pressurize the growing crack. This aspect is considerably more significant since it determines the loss of resisting cross-section and rebar protection.

ACKNOWLEDGEMENT

This work was developed in the framework of the PhD project “Severe Spalling in concrete exposed to Fire” supported by SFIC (Professional Syndicate of the French Cement Industry).

REFERENCES

[1] C.R. Gagg, Cement and concrete as an engineering material: An historic appraisal and case study analysis, Eng. Fail. Anal. 40 (2014) 114–140.

[2] J.-C. Liu, K.H. Tan, Y. Yao, A new perspective on nature of fire-induced spalling in concrete, Constr. Build. Mater. 184 (2018) 581–590.

[3] M. Maier, M. Zeiml, R. Lackner, On the effect of pore-space properties and water saturation on explosive spalling of fire-loaded concrete, Constr. Build. Mater. 231 (2020) 117150.

[4] Y. Ichikawa, Prediction of Pore Pressures , Heat and Moisture Transfer Leading to Spalling of Concrete during Fire, PhD. Thesis. 1 (2000).

[5] M. Ozawa, H. Morimoto, Effects of various fibres on high-temperature spalling in high-performance concrete, Constr. Build. Mater. 71 (2014) 83–92.

[6] Y. Ichikawa, G.L. England, Prediction of moisture migration and pore pressure build-up in concrete at high temperatures, Nucl. Eng. Des. 228 (2004) 245–259.

[7] M.B. Dwaikat, V.K.R. Kodur, Hydrothermal model for predicting fire-induced spalling in concrete structural systems, Fire Saf. J. 44 (2009) 425–434.

[8] F. Robert, L. Bisby, F.T. Centre, Fire Spalling of Concrete : Experimental Parametric Study and Numerical Modelling, in: 4th Int. Work. Concr. Spalling Due to Fire Expo., Leipzig, 2015: pp. 1–9.

[9] J. Zhao, J.J. Zheng, G.F. Peng, K. Van Breugel, A meso-level investigation into the explosive spalling mechanism of high-performance concrete under fire exposure, Cem. Concr. Res. 65 (2014) 64–75.

[10] H.L. Zhang, C.T. Davie, A numerical investigation of the influence of pore pressures and thermally induced stresses for spalling of concrete exposed to elevated temperatures, Fire Saf. J. 59 (2013) 102–110.

[11] F. Lo Monte, F. Lombardi, R. Felicetti, M. Lualdi, Ground-Penetrating Radar monitoring of concrete at high temperature, Constr. Build. Mater. 151

(2017) 881–888.
[12] Yavus Sertmehmetoglu, On a mechanism of spalling of concrete under fire conditions, university of London, king’s college, 1977.
[13] J.-C. Mindeguia, P. Pimienta, H. Carré, C. La Borderie, Experimental study on the contribution of pore vapour pressure to the thermal instability risk of concrete, in: 1St Int. Work. Concr. Spalling Due To Fire Expo., 2009: pp. 150–167.
[14] F. Lo Monte, R. Felicetti, M.J. Miah, The influence of pore pressure on fracture behaviour of Normal-Strength and High-Performance Concretes at high temperature, Cem. Concr. Compos. 104 (2019) 103388.
[15] Y. Fu, L. Li, Study on mechanism of thermal spalling in concrete exposed to elevated temperatures, Mater. Struct. Constr. 44 (2011) 361–376.
[16] F. Lo Monte, P.G. Gambarova, Corner spalling and tension stiffening in heat-damaged R/C members: a preliminary investigation, Mater. Struct. Constr. 48 (2015) 3657–3673.
[17] R. Felicetti, Assessment of a fire damaged concrete overpass: the Verona bus crash case study, (2020).
[18] M. Zeiml, R. Lackner, H.A. Mang, Experimental insight into spalling behavior of concrete tunnel linings under fire loading, Acta Geotech. 3 (2008) 295–308.
[19] D. Gawin, F. Pesavento, B.A. Schrefler, Towards prediction of the thermal spalling risk through a multi-phase porous media model of concrete, Comput. Methods Appl. Mech. Eng. 195 (2006) 5707–5729.
[20] D. Gawin, F. Pesavento, A.G. Castells, On reliable predicting risk and nature of thermal spalling in heated concrete, Arch. Civ. Mech. Eng. 18 (2018) 1219–1227.
[21] R. Yarmohammadian, R. Felicetti, F. Robert, L. Izoret, The role of moisture on crack instability of spalling concrete, in: 7th Int. Work. Concr. Spalling Due to Fire Expo., n.d.: p. 108.
[22] R. Felicetti, F. Lo Monte, P. Pimienta, A new test method to study the influence of pore pressure on fracture behaviour of concrete during heating, Cem. Concr. Res. 94 (2017) 13–23.